Title

Exploring substrate/ionomer interaction under oxidizing and reducing environments

Authors

Tesfaye, Meron

MacDonald, Andrew N

Dudenas, Peter J

et al.

Publication Date

2018-02-01

DOI

10.1016/j.elecom.2018.01.004

Exploring substrate/ionomer interaction under oxidizing and reducing environments

Meron Tesfaye,[a, b] Andrew MacDonald,[a] Peter J. Dudenas,[a, b] Ahmet Kusoglu,[b] Adam Z. Weber[b,*]

[a] Department of Chemical and Biomolecular Engineering, University of California, Berkeley, CA, 94720, USA

[b] Energy Technologies Area, Lawrence Berkeley National Laboratory (LBNL), Berkeley, CA, 94720, USA

* Author to whom correspondence should be addressed. azweber@lbl.gov

Graphical Abstract

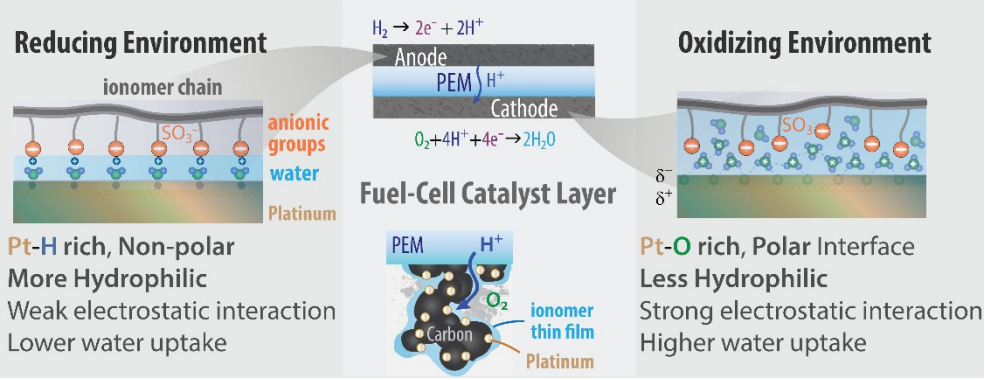

Keywords:

Hydrogen; Fuel cell; Ionomer; Confinement; Thin film; Water uptake

Highlight:

- Revealed swelling of ionomer thin-film on Pt in H_2 for the 1st time.
- Demonstrated lower swelling of ionomer on both Pt and Si/SiO_2 under H_2 gas.
- Observed densification in ionomer thin-film under H_2 environment via GISAXS.
- Thin-film swelling dynamics is surface/ionomer interaction dependent.
- Polarity and hydrophilicity are key factors in Pt interface/ionomer interaction.

Abstract

Local gas transport limitation attributed to the ionomer thin-film in the catalyst layer is a major deterrent to widespread commercialization of polymer-electrolyte fuel cells. So far functionality and limitations of these thin-films have been assumed identical in the anode and cathode. In this study, Nafion thin-films on platinum(Pt) support were exposed to H_2 and air as model schemes, mimicking anode and cathode catalyst layers. Findings indicate decreased swelling, increased densification of ionomer matrix, and increased humidity-induced aging rates in reducing environment, compared to oxidizing and inert environments. Observed phenomenon could be related to underlying Pt-gas interaction dictating Pt-ionomer behavior. Presented results could have significant implications about the disparate behavior of ionomer thin-film in anode and cathode catalyst layers.

1. Introduction

As polymer-electrolyte fuel cells (PEFCs) gain traction in the energy-device landscape, they face a major hurdle from significant mass-transport losses associated with the ionomer/catalyst interface [1], [2]. Sources of mass-transport losses include: confinement driven gas transport losses in ionomer thin-film coating carbon-supported platinum, interfacial resistances caused by structural changes at local ionomer-platinum boundary, and partial electrochemical deactivation of platinum surfaces [3]–[6]. The latter can impact overall kinetics on platinum(Pt) surfaces [7], [8], however such effects on ionomer mass-transport and the interplay with reducing atmospheres are unknown. As a result, explicit understanding of losses at the ionomer/Pt interface is required for optimal electrode-ionomer design and accelerating market penetration of PEFCs.

Ionomer thin-films cast onto a Pt surface can serve as model systems providing a focused glimpse into the catalyst layer. Although bulk, continuous polycrystalline Pt does not fully describe Pt nanoparticle phenomenon present in real catalyst layers, it can still elucidate surface specific interactions that impact ionomer properties and morphology [9], [10]. While impact of Pt substrate on ionomer performance have been shown [8], [11], efforts to clarify the source of this impact have been contradictory, especially in elucidating the role of water on oxidized and unoxidized Pt surfaces [12], [13]. Additionally, the extent of Pt surface influence on ionomer during exposure to oxidative/reductive environments remains unexplored. In this study, water-vapor-sorption dynamics of dispersion-cast Nafion thin-films under reducing (H_2), oxidizing (Air), and inert (Ar, N_2) environments are investigated in order to understand the Pt/ionomer interaction in anode and cathode catalyst layers.

2. Material and Methods

2.1. Thin-film Preparation

Nafion dispersions (5 wt%, 1100 g/mol SO_3^- equivalent-weight, Sigma Aldrich) were diluted in isopropanol, spin cast onto Pt-coated Si, and Si/SiO_2 wafers to form ~50 nm films. Pt substrates were prepared via e-beam evaporation of 5nm Ti adhesion layer followed by 60nm of Pt. Pt substrates were cleaned with benchtop Ar plasma for 6 minutes prior to casting. Thin-films were annealed at 150°C under vacuum for 1 hr before measurement.

2.2. Water-Uptake Measurement

Thickness change of Nafion films was monitored using *in-situ* spectroscopic ellipsometry (J.A. Woollam) as detailed in Ref [14]. Measurements shown are the average of at least two separate samples measured <15 minutes after annealing. To create a consistent water history, all measurements were preceded with an hour exposure to dry (0%) and saturated (96%) relative humidity (RH) (See Fig 1a for hydration protocol). Humidity-dependent thickness (*L(t,RH)*) was an average of the last 10 min of set humidity. The % change from dry (L_o) is given by:

$$Change \in Thickness\,(\,) = 100 \times \frac{L(t, RH) - L_o}{L_o} \qquad (1)$$

2.3. Grazing Incidence Small Angle Scattering (GISAXS) Measurements

Pt-coated Nafion films were placed into an in-house built environmental chamber with X-ray transparent Kapton windows as in Ref [6]. The sample was equilibrated in dry H_2 and N_2 gas at room temperature and GISAXS patterns were collected after multiple purges for 5 to 10 minutes in each gas, at varying incidence angles (α_i).

2.4. Mechanical-Property Measurement

100 nm Nafion films were prepared on Pt-coated thin Si cantilever wafers (105μm thickness by approximately 0.5cm x 4cm). Sample was clamped in an environmental cell with humidified

gas feeds. Constrained swelling due to the substrate results in a compressive force, which bends the Si cantilever. Using a laser array reflected off the backside of sample, change in curvature of the cantilever was measured and related to stress-thickness via Stoney's equation, see Ref [15]. Humidity-induced stress-strain curves were generated by combining stress and strain (from ellipsometry, see Equation 1) under the same humidity conditions, and the deformation energy density was calculated by integrating the area under the curve.

3. Results and Discussion

Figure 1b compares swelling of ionomer films on Pt and Si/SiO_2 under different humidified gas feeds. Swelling values demonstrate a depression in swelling for ionomer thin-films exposed to H_2. The authors note values reported here fall between previous studies [13, 16]. Differences in swelling values between studies are ascribed to different ageing, conditioning, and annealing protocols.

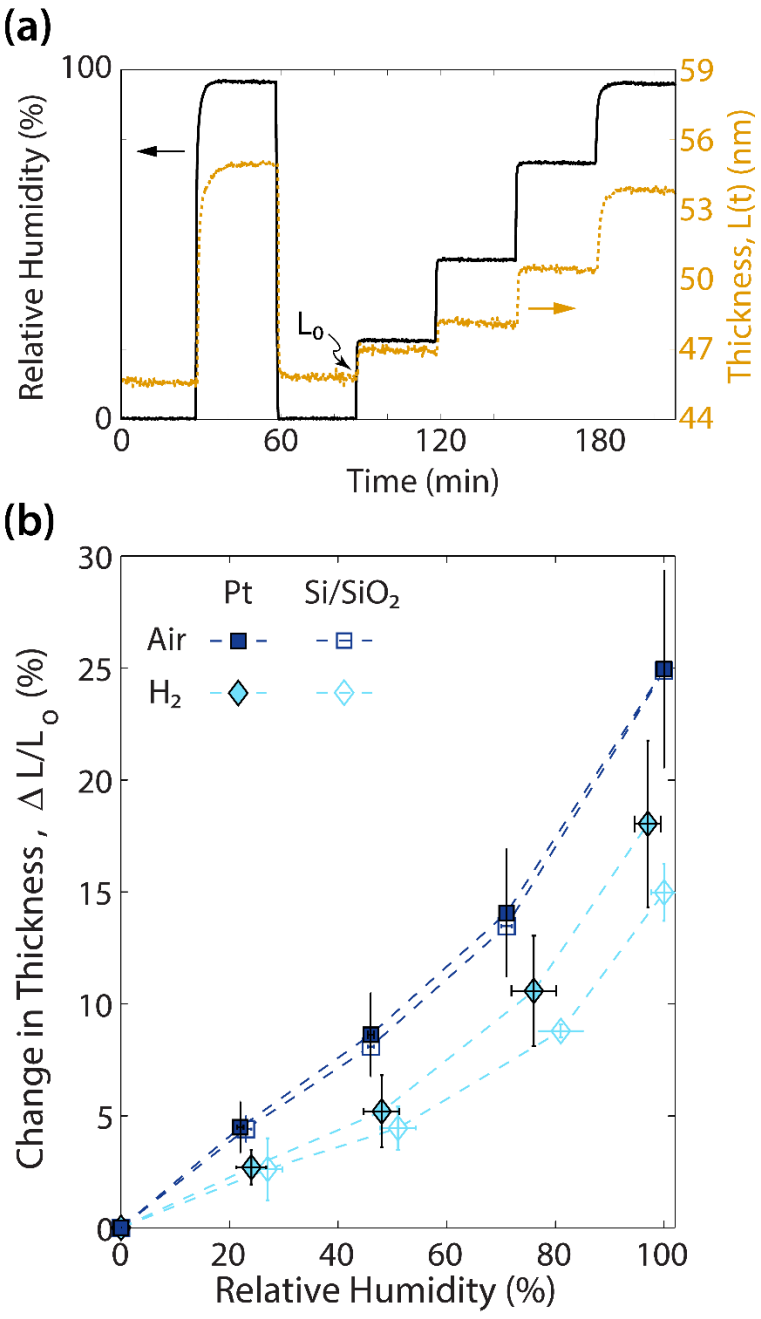

Figure 1: (a) Humidity protocol applied during in-situ tracking of spin-cast Nafion thin-films (~50 nm) (b) % Change in thickness on Pt and Si/SiO_2 substrate under H_2 and Air environments as a function of relative-humidity.

The reversibility and persisting impact of the gaseous environment on ionomer swelling was explored using humidity-cycling by alternating inert and reducing gas exposure. *In-situ* ionomer thickness change on Pt was monitored over three hydration cycles: first, a single step of dry to 96% RH gas exposure (Cycle 0, gas 1); second, humidity was stepped down to 0% RH prior to hydration cycling (Cycle 1, gas 1); finally, gas 1 was switched and stepped RH was applied (Cycle 2, gas 2). Here, the dry reference thickness was set to the thickness from Cycle 0. Figure 2a shows difference in swelling in each gas combination under dry conditions, i.e., $(L_{Dry} - L_{o,\,Cycle\,0})/L_{o,\,Cycle\,0}$. Humidity-cycling under inert gas environment (Ar → Ar → Ar) displays minimal thickness hysteresis from start to finish. However, cycling in H_2 only (H_2 → H_2 → H_2) and H_2 then Ar (H_2 → H_2 → Ar) introduces a continual increase in dry thickness upon repeated cycling. Swelling in Ar then H_2 (Ar → Ar → H_2) demonstrates a large relative shift in dry thickness immediately after H_2 exposure. Figure 2b shows swelling under saturated (96% RH) conditions for each gas combination, i.e. $(L_{Saturated} - L_{Saturated,\,Cycle\,0})/L_{o,\,Cycle\,0}$. The thickness change in humid inert gas environment (Ar → Ar → Ar) is maintained despite repeated relaxation and tension introduced by changes in humidity. However, RH cycling in both H_2 only (H_2 → H_2 → H_2) and H_2 then Ar (H_2 → H_2 → Ar) reduces the maximum water-uptake capacity. A reducing environment not only diminishes water uptake successively upon cycling, but does so to a greater extent than an inert environment. Switching order of H_2 and Ar (H_2 → H_2 → Ar versus Ar → Ar → H_2) exhibits a reduction in swelling under saturated

conditions at a rate that is between that of H_2- and Ar-only environments, confirming the impact of the H_2 environment.

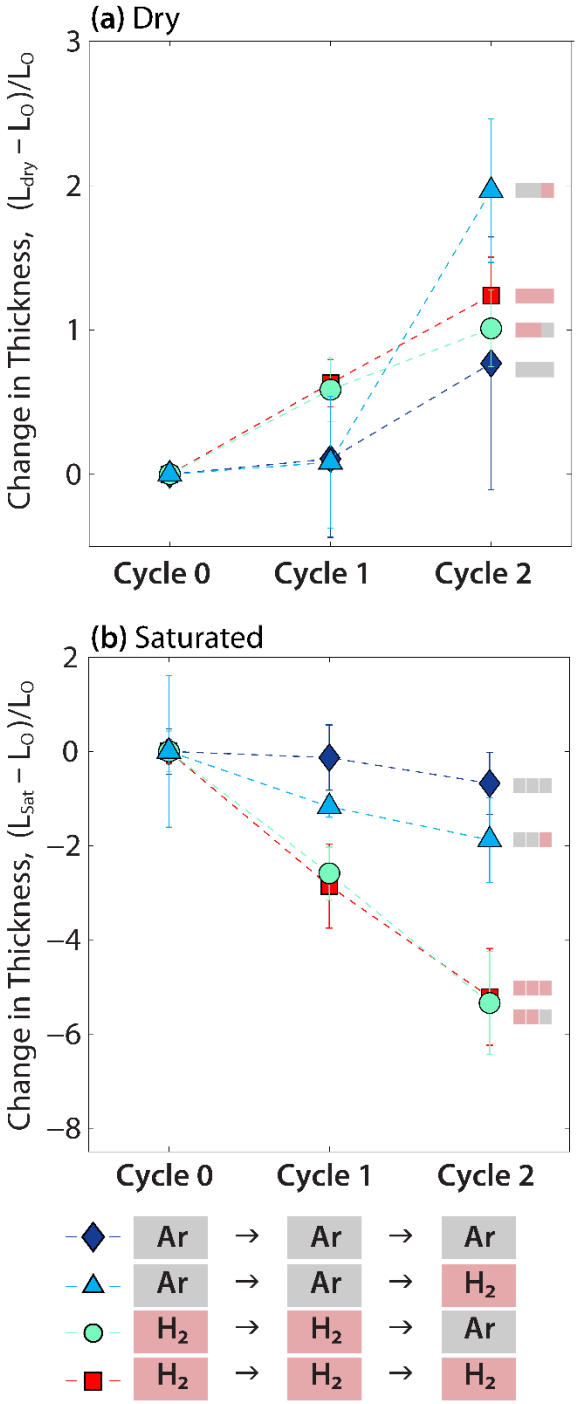

Figure 2: Humidity-cycling of Pt-supported Nafion thin-films (~50 nm) with alternating inert and reducing gas. Comparison of Cycle 1 in gas 1 and Cycle 2 in alternative gas 2.

Thickness change in (a) Dry and (b) Saturated (96% RH) relative to dry and saturated thickness in Cycle 0 exposed to gas 1, respectively.

The findings in Fig. 1 and 2 are consequences of changes at the ionomer/Pt interface induced by gas/Pt interaction. Surface oxidation on Pt metal can occur via electrochemical and thermochemical pathways [17]. In a thermochemically oxidized Pt surface, exposure to an oxidative gaseous environment like air will enlarge oxidized metal islands on Pt, while exposure to a reducing environment like H_2 can reduce the unstable passivated surface even under ambient conditions [17]–[20]. Pt substrates in this study are likely to exist with some surface oxidation as they are stored under ambient conditions. This oxide surface continues to grow with continued exposure to an oxidizing environment or, is reduced and saturated with dissociated atomic hydrogen during H_2 exposure; a phenomenon that has been reported experimentally and computationally [10], [21]–[23]. As a result, during exposure to Air and H_2, Pt interface can exist at varied states of oxidation and reduction resulting in sample-to-sample variability. Nonetheless, adsorbed hydrogen reduces the solid-surface free energy [21], resulting in a more hydrophilic but nonpolar Pt/H interface compared with that of oxidized Pt. This phenomenon was verified by using bare Pt-coated crystal in a quartz-crystal microbalance, which exhibited significant adsorption of H_2 on Pt surface when dry, and greater absorption of water when saturated due to greater affinity for water at the Pt/H interface (data not shown). The Pt/H interface lacks strong electrostatic interactions, resulting in possible ionomer restructuring to orient hydrophilic sidechains towards the Pt/H interface, where water molecules are likely to gather, thereby creating a dense region of hydrophobic ionomer away from the interface. In such a scenario, the bulk of the ionomer behaves like a higher equivalent-weight ionomer with lower water uptake.

On the other hand, negatively charged oxygen atoms on an oxidized Pt surface, which, while comparatively less hydrophilic, induce a strong polar dipole and enhance electrostatic interactions between hydronium ions and sulfonic-acid moieties. Similar depression in water-vapor uptake in thin-films on Si/SiO_2 support under H_2 also point towards impact of oxidized surfaces. Under ambient conditions, growth of native oxide layer of 1 to 2 nm is expected on a Si substrate. Continued layer-by-layer growth of SiO_2; however, requires presence of both water and oxygen [24], [25]. Although reduction of the oxide layer is not occurring under H_2 environment on Si/SiO_2 support, oxide formation is actively being facilitated under humidified air. These interactions enhance the overall effective water uptake within the ionomer on oxidized surface, which is consistent with predictions from molecular-dynamics simulations [26]. Figure 3 schematically portrays the balancing impacts of polarity and hydrophilicity in reducing and oxidizing environment.

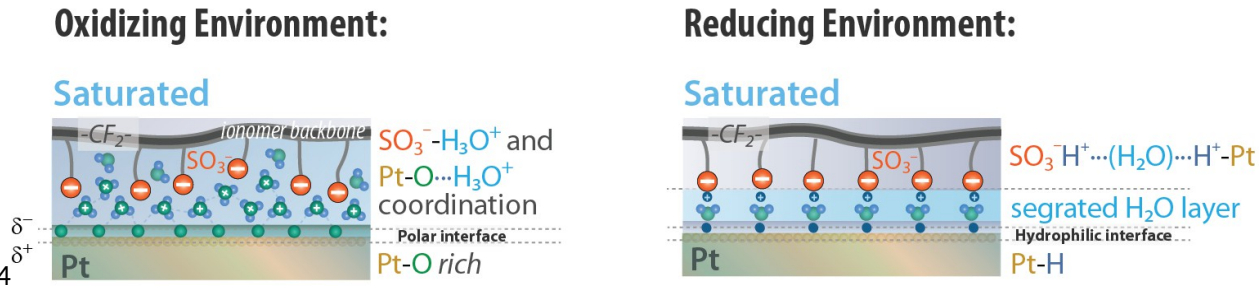

Figure 3: Schematic representation of platinum(Pt)/ionomer thin-film interface impact in oxidizing and reducing environment resulting from differences in polarity and hydrophilicity.

The above hypothesis is supported by morphological changes tracked by GISAXS and mechanical response of Nafion thin-film on Pt exposed to H_2 and N_2 gases. When α_i of x-ray

beam is below the critical angle of the polymer film, $\alpha_{c,film}$, total external reflection occurs with a surface-sensitive scattering [27], whereas above $\alpha_{c,film}$, , the x-ray beam penetrates through the entire film and scattering from the paracrystalline Pt surface is observed. As shown in Figure 4a, the paracrystalline peak is present at α_i = 0.16 in dry N_2, but does not appear until α_i = 0.18 in dry H_2, indicating an increase in the ionomer's critical angle, which is a function of chemical structure and density. This positive shift in α_c points to restructuring of the ionomer, including possible rearrangement of the hydrogen bonding of sidechains near the Pt/H interface, resulting in a more effectively packed, dense, hydrophobic ionomer structure. In addition, mechanical stress generated in thin film during its humidification in H_2 and N_2 is measured on a cantilever beam. When this stress is plotted against thickness swelling measured separately at the same RHs, shown in Fig 4b, a curve is generated, the area under which demonstrates lower deformation energy density accumulated in the film in H_2 than N_2 (539 versus 680 kJ/m^3). This provides further evidence to the more hydrophilic but weakly-interacting Pt/H interface induced by H_2, creating a water-rich layer (see Figure 3), thereby resulting in a reduced translation of ionomer deformation onto the substrate.

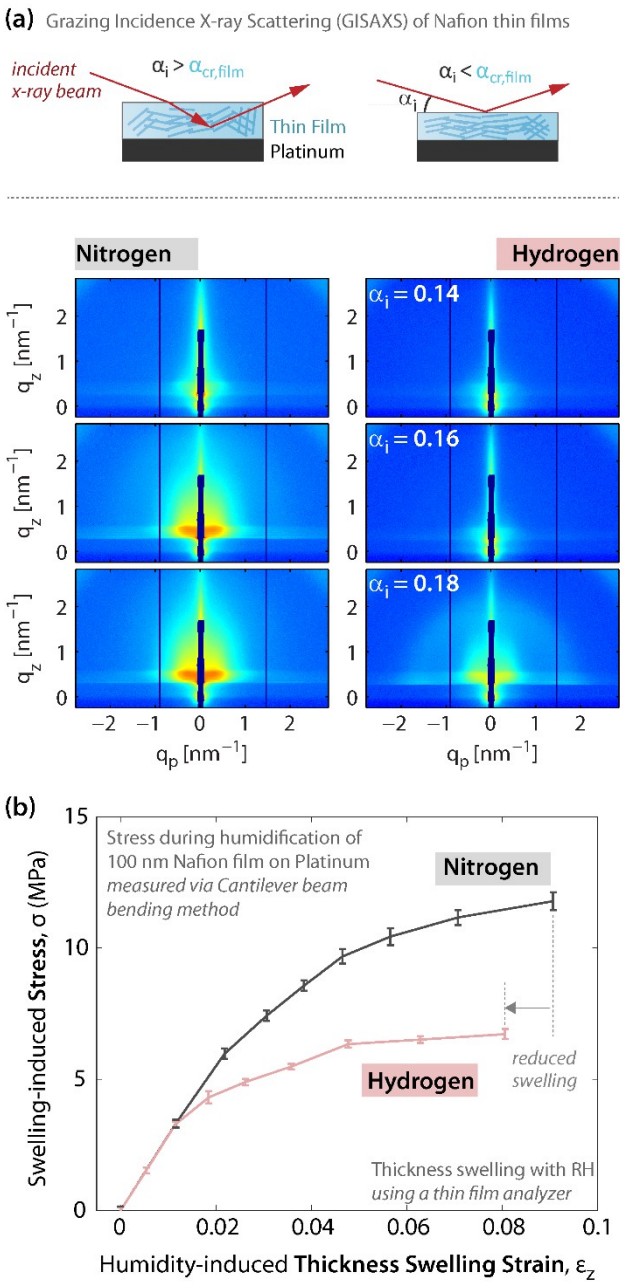

Figure 4: (a) 2D GISAXS pattern of Pt-supported Nafion thin-films (~50 nm) equilibrated in dry N_2 and H_2 gas. The paracrystalline peak visibility shifts from $\alpha_i \geq 0.16$ in N_2 to $\alpha_i \geq 0.18$ in H_2. (b) Swelling-induced stress in the thin film measured via cantilever

method during humidification in N_2 and H_2 plotted against the thickness swelling of the film.

Despite being the least understood component, the gas/ionomer/Pt interface in the catalyst layer bears the utmost duty for PEFC performance. Thus, there is need for greater understanding of pairwise interaction between gas/ionomer, ionomer/Pt, and gas/Pt interfaces to reduce critical transport losses and improve electrode design. To that effect, this study focused on how gas/Pt interaction impacts Pt surface and ionomer thin-film morphology and properties. Unexpectedly, a reduced swelling, increased densification, decreased deformation energy density and continual reduction in effective water uptake in the ionomer during cycling were observed under H_2 relative to oxidizing or inert environment. These observations demonstrate the coupled impact of gas/substrate and ionomer/substrate interactions on ionomer thin-film's behavior and ultimately it's transport properties [28]. Therefore, there is a need for increased electrode-specific investigations and separate ionomer design for anode and cathode catalyst layers. The impact of electronic potential going from oxidation to reduction potentials can also affect the surface-state identity and ionomer thin-film morphology, which is a focus of current research. Furthermore, existence of a water-rich phase at the Pt/ionomer interface in a reducing environment can impact surface conductivity significantly, which may not occur in an oxidizing environment. The findings herein also indicate heightened vulnerability to delamination of ultra-thin ionomer films in the anode due to increased water-layer thickness and reduced deformation energy density.

Acknowledgements

This work was funded in part by the National Science Foundation (Grant No. DGE-1106400) and the Fuel Cell Performance and Durability Consortium, by the Fuel Cell Technologies Office, Office of Energy Efficiency and Renewable Energy, of the U.S. Department of Energy (Contract No. DE-AC02-05CH11231). This work made use of facilities at the Advanced Light Source beamline 7.3.3, supported by the Office of Science, Office of Basic Energy Sciences, of the U.S. Department of Energy (Contract No. DE-AC02-05CH11231).

References

[1] U. Beuscher, “Experimental Method to Determine the Mass Transport Resistance of a Polymer Electrolyte Fuel Cell,” *J. Electrochem. Soc.*, vol. 153, no. 9, p. A1788, 2006.

[2] A. Kongkanand and M. F. Mathias, “The Priority and Challenge of High-Power Performance of Low- Platinum Proton-Exchange Membrane Fuel Cells,” *J. Phys. Chem. Lett.*, vol. 7, pp. 1127–1137, 2016.

[3] A. Z. Weber and A. Kusoglu, “Unexplained Transport Resistances for Low-Loaded Fuel-Cell Catalyst Layers,” *J. Mater. Chem. A*, vol. 2, no. c, pp. 17207–17211, 2014.

[4] R. Jinnouchi, K. Kudo, N. Kitano, and Y. Morimoto, “Molecular Dynamics Simulations on O2 Permeation through Nafion Ionomer on Platinum Surface,” *Electrochim. Acta*, vol. 188, pp. 767–776, 2016.

[5] A. Ohira, S. Kuroda, H. F. M. Mohamedz, and B. Tavernier, “Effect of interface on surface morphology and proton conduction of polymer electrolyte thin films,” *Phys. Chem. Chem. Phys. Phys. Chem. Chem. Phys*, vol. 15, pp. 11494–11500, 2013.

[6] A. Kusoglu, D. Kushner, D. K. Paul, K. Karan, M. a. Hickner, and A. Z. Weber, “Impact of Substrate and Processing on Confi nement of Nafi on Thin Films,” *Adv. Funct. Mater.*, vol. 24, no. 30, pp. 4763–4774, Aug. 2014.

[7] N. P. Subramanian, T. A. Greszler, J. Zhang, W. Gu, and R. Makharia, “Pt-Oxide Coverage-Dependent Oxygen Reduction Reaction (ORR) Kinetics,” *J. Electrochem. Soc.*, vol. 159, no. 5, pp. 531–540, 2012.

[8] J. Chlistunoff and B. Pivovar, “Effects of Ionomer Morphology on Oxygen Reduction on Pt,” *J. Electrochem. Soc.*, vol. 162, no. 8, pp. F890–F900, 2015.

[9] H. A. Gasteiger, S. S. Kocha, B. Sompalli, and F. T. Wagner, “Activity benchmarks and

requirements for Pt, Pt-alloy, and non-Pt oxygen reduction catalysts for PEMFCs," *Appl. Catal. B Environ.*, vol. 56, no. 1–2 SPEC. ISS., pp. 9–35, 2005.

[10] L. Gai, Y. K. Shin, M. Raju, A. C. T. Van Duin, and S. Raman, "Atomistic adsorption of oxygen and hydrogen on platinum catalysts by hybrid grand canonical monte carlo/reactive molecular dynamics," *J. Phys. Chem. C*, vol. 120, no. 18, pp. 9780–9793, 2016.

[11] Y. Ono and Y. Nagao, "Interfacial Structure and Proton Conductivity of Nafion at the Pt-Deposited Surface," *Langmuir*, vol. 32, no. 1, pp. 352–358, Jan. 2016.

[12] D. L. Wood, J. Chlistunoff, J. Majewski, and R. L. Borup, "Nafion structural phenomena at platinum and carbon interfaces.," *J. Am. Chem. Soc.*, vol. 131, no. 50, pp. 18096–104, Dec. 2009.

[13] C. F. Murthia, V.S., Dura, J.A, Satijab , S., Majkrzakb, "Water Uptake and Interfacial Structural Changes of Thin Film Nafion ® Membranes Measured by Neutron Reflectivity for PEM Fuel Cells," *Trans. E C S Soc. Electrochem.*, vol. 16, no. 2, pp. 1471–1485, 2008.

[14] M. A. Modestino *et al.*, "Self-Assembly and Transport Limitations in Con fi ned Na fi on Films," *Macromolecules*, vol. 46, p. 867−873, 2013.

[15] K. A. Page *et al.*, "In Situ Method for Measuring the Mechanical Properties of Nafion Thin Films during Hydration Cycles," *ACS Appl. Mater. Interfaces*, vol. 7, no. 32, pp. 17874–17883, 2015.

[16] A. Kusoglu and A. Z. Weber, "New Insights into Perfluorinated Sulfonic-Acid Ionomers," *Chem. Rev.*, vol. 117, no. 3, pp. 987–1104, 2017.

[17] H. Luo, S. Park, H. Yeung, H. Chan, and M. J. Weaver, "Surface Oxidation of Platinum-Group Transition Metals in Ambient Gaseous Environments: Role of Electrochemical

versus Chemical Pathways," *J. Phys. Chem. B*, vol. 104, pp. 8250–8258, 2000.

[18] J. L. Gland, "Molecular and atomic adsorption of oxygen on the Pt(111) and Pt(S)-12(111) × (111) surfaces," *Surf. Sci.*, vol. 93, no. 2–3, pp. 487–514, Mar. 1980.

[19] J. L. Gland and V. N. Korchak, "THE ADSORPTION OF OXYGEN ON A STEPPED PLATINUM SINGLE CRYSTAL SURFACE," *Surf. Sci.*, vol. 75, pp. 733–750, 1978.

[20] R. W. McCabe, C. Wong, and H. S. Woo, "The passivating oxidation of platinum," *J. Catal.*, vol. 114, no. 2, pp. 354–367, 1988.

[21] Q. Shi and R. Sun, "Adsorption manners of hydrogen on Pt(100), (110) and (111) surfaces at high coverage," *Comput. Theor. Chem.*, vol. 1106, pp. 43–49, 2017.

[22] V. H. Baldwin and J. B. Hudson, "Coadsorption of Hydrogen and Carbon Monoxide on (111) Pt," *J. Vac. Sci. Technol.*, vol. 8, no. 1, pp. 49–52, 1971.

[23] K. Christmann, G. Ertl, and T. Pignet, "Adsorption of hydrogen on a Pt(111) surface," *Surf. Sci.*, vol. 54, no. 2, pp. 365–392, 1976.

[24] M. Morita, E. Ohmi, E. Hasegawa, M. Kawakami, and K. Suma, "Control factor of native oxide growth on silicon in air or in ultra pure water," *Appl. Phys. Lett.*, vol. 55, no. 6, pp. 562–564, 1989.

[25] M. Morita, T. Ohmi, E. Hasegawa, M. Kawakami, and M. Ohwada, "Growth of native oxide on a silicon surface," *J. Appl. Phys.*, vol. 68, no. 3, pp. 1272–1281, 1990.

[26] Q. He, N. S. Suraweera, D. C. Joy, and D. J. Keffer, "Structure of the Ionomer Film in Catalyst Layers of Proton Exchange Membrane Fuel Cells," *J. Phys. Chem. C*, vol. 117, no. 48, pp. 25305–25316, 2013.

[27] P. Muller-Buschbaum, "A Basic Introduction to Grazing Incidence Small Angle X-Ray Scattering," in *Applications of Synchrotron Light to Scattering and Diffraction in*

Materials and Life Sciences., vol. 776, 2009, pp. 61–89.

[28] A. Kusoglu, T. J. Dursch, and A. Z. Weber, “Nanostructure/Swelling Relationships of Bulk and Thin-Film PFSA Ionomers,” *Adv. Funct. Mater.*, vol. 26, no. 27, pp. 4961–4975, 2016.